Interaction of Vinblastine with Calf Brain Tubulin: Multiple Equilibria†

George C. Na‡ and Serge N. Timasheff*
Graduate Department of Biochemistry, Brandeis University, Waltham, Massachusetts 02254
Received January 17, 1986; Revised Manuscript Received May 28, 1986

ABSTRACT: The binding of the anticancer drug vinblastine to calf brain tubulin was measured by a batch gel filtration method in PG buffer (0.01 M NaP_i, 10^{-4} M GTP, pH 7.0) at three different protein concentrations. The Scatchard binding isotherms obtained were curvilinear. The binding of the first vinblastine molecule to each tubulin α–β dimer (M_r 110000) was enhanced by an increase in the protein concentration. Additional binding of vinblastine to the protein was independent of the protein concentration. Theoretical ligand binding isotherms were calculated for a ligand-induced macromolecule self-association involving various ligand stoichiometries and association schemes. Fitting of the experimental data to these isotherms showed that the system can be described best by a one-ligand-induced isodesmic indefinite self-association. The pathway giving the best fit consists of a ligand-mediated plus -facilitated self-association mechanism. The self-association-linked bound vinblastine binds specifically at a site with an intrinsic binding constant $K_1 = 4 \times 10^4$ M^{-1}. Additional vinblastine molecules can bind less strongly to tubulin in probably nonspecific fashion, and the previous reports of two specific sites on α–β tubulin for binding vinblastine are incorrect. The self-association constant K_2 for liganded tubulin is 1.8×10^5 M^{-1}. This analysis is fully consistent with the conclusions derived earlier from the linked function analysis of the vinblastine-induced tubulin self-association [Na, G. C., & Timasheff, S. N. (1980) *Biochemistry 19*, 1347–1354; Na, G. C., & Timasheff, S. N. (1980) *Biochemistry 19*, 1355–1365].

Vinblastine and vincristine are two vinca alkaloids that have been used extensively in cancer chemotherapy. Their antineoplastic activity stems mainly from their ability to disrupt cell microtubules, causing the dissolution of cell mitotic spindles and the arrest of the cells at their metaphase. At high dosages, these drugs can induce in cells the formation of highly ordered tubulin paracrystalline aggregates that contain equimolar amounts of the drug and of tubulin (Bensch & Malawista, 1968, 1969; Malawista & Sato, 1969; Bryan, 1971, 1972a,b; Wilson et al., 1978).

In vitro studies from three independent laboratories have resulted in a consensus that each tubulin α–β dimer contains two strong vinblastine binding sites (Lee et al., 1975; Wilson et al., 1975; Bhattacharyya & Wolff, 1976). However, widely divergent association constants, ranging from 2×10^4 M^{-1} to 6×10^6 M^{-1}, were reported for these sites.

In PG[1] buffer, purified calf brain tubulin binds vinblastine and undergoes a stepwise indefinite self-association (Weisenberg & Timasheff, 1970; Na & Timasheff, 1980a). Analysis of the tubulin self-association as a function of vinblastine concentration has shown that each step of the protein self-association is accompanied by the binding of one vinblastine molecule. Curve fitting analysis resulted in equilibrium constants of 1.8×10^4 M^{-1} for the binding of vinblastine to tubulin α–β dimers and 1.8×10^5 M^{-1} for the association between two liganded α–β dimers (Na & Timasheff, 1980b). Most important, these studies demonstrated that the binding of vinblastine to tubulin and the drug-induced self-association of the protein are two thermodynamically linked events. For such a ligand-induced protein self-association system, there should be a mutual dependence between the apparent strengths of ligand binding and of protein self-association. Consequently, analysis of the ligand binding isotherms must take into consideration the presence of the equilibrium linkage, and it is the failure to recognize this factor that could be the reason for the discrepancy between the reported drug binding constants. We have measured, therefore, the binding of vinblastine to tubulin under equilibrium conditions as a function of tubulin concentration. The results were analyzed with full cognizance of the equilibrium linkage. Preliminary reports of this work have been presented earlier (Na & Timasheff, 1980c, 1981b).

Materials and Methods

The guanosine 5′-triphosphate (GTP)[1] used was grade II-S from Sigma.[2] Special ultrapure grade ammonium sulfate and sucrose were obtained from Schwarz/Mann. Ultrapure guanidine hydrochloride (Gdn-HCl)[1] was purchased from Heico Co., and its solution was filtered through a sintered glass funnel to remove insoluble debris before use. Bio-Gel P-100 was from Bio-Rad Laboratory and Blue Dextran 2000 was from Pharmacia Fine Chemicals. Vinblastine sulfate was a gift from Eli Lilly and Co., through the courtesy of Dr. K. Gerzon. [^{3}H]Vinblastine was purchased from Amersham Company. All other chemicals used were reagent grade.

Preparation of Calf Brain Tubulin. Tubulin was prepared from the brains of freshly slaughtered calves by using the modified Weisenberg method (Weisenberg et al., 1968; Weisenberg & Timasheff, 1970; Lee et al., 1973). The procedure was further modified by using 0.5 mM $MgCl_2$ instead of 5 mM $MgCl_2$ throughout the preparation, and a sintered glass funnel of coarse porosity was used in place of centrifugation to separate the solution from the DEAE-Sephadex gel.

† This work was supported in part by NIH Grants CA-16707 and GM-14603. This paper is Publication No. 1593 from the Graduate Department of Biochemistry, Brandeis University.
‡ Present address: U.S. Department of Agriculture, Agricultural Research Service, Eastern Regional Research Center, Philadelphia, PA 19118.

[1] Abbreviations: PG, 0.01 M NaP_i, 10^{-4} M GTP, pH 7.0; PMG, 0.01 M NaP_i, 5×10^{-4} M $MgCl_2$, 10^{-4} M GTP, pH 7.0; Gdn-HCl, guanidine hydrochloride; GTP, guanosine 5′-triphosphate.

[2] Reference to brand or firm name does not constitute endorsement by the U.S. Department of Agriculture over others of a similar nature not mentioned.

0006-2960/86/0425-6214$01.50/0

The tubulin obtained was stored in 1 M sucrose–PMG buffer[1] (0.01 M NaP_i, 5×10^{-4} M $MgCl_2$, and 10^{-4} M GTP, pH 7.0) under liquid nitrogen until use (Frigon & Lee, 1972). Before each experiment, the tubulin was thawed and brought to equilibration with the experimental buffer through a batch gel filtration step and then a column gel filtration step on Sephadex G-25. Between the two gel filtrations, the solution was centrifuged at 40000*g* for 30 min to remove aggregates (Na & Timasheff, 1982). The protein concentration was calculated from its absorbance in 6 M Gdn-HCl by using an extinction coefficient of 1.03 mL mg^{-1} cm^{-1} at 275 nm (Na & Timasheff, 1981a).

Determination of Vinblastine Binding to Tubulin. The binding of vinblastine to tubulin was measured by a batch gel filtration technique (Fasella et al., 1965; Pearlman & Crêpy, 1967; Hirose & Kano, 1971). Forty milligrams of the dried gel (Bio-Gel P-100) was weighed in each 12 × 75 mm borosilicate culture tube. To each tube was then added 0.5–0.6 g of the experimental buffer. After tightly sealing the tubes with parafilm, the gel was allowed to swell for 20 h at room temperature. At the end of the swelling, 0.2 g of PG buffer containing a known concentration of [^{3}H]vinblastine was added, and the gel was mixed gently. This was followed by addition of 0.2 g of tubulin stock solution that had been preequilibrated with PG buffer. The complete mixture was incubated at 20 °C with gentle shaking for 1 h. After the incubation, the gel was allowed to settle to the bottom of the test tube, and aliquots were carefully taken from the supernatant for liquid scintillation radioactivity counting and measurement of tubulin concentration. Controls were treated identically as the samples. They contained the same mixture, except that buffer was substituted for either the protein or the vinblastine solution. The first control gave the adsorption of vinblastine to the gel matrix, while the second control gave the excluded volume of the gel with respect to tubulin. Throughout the experiment, all aliquots were measured gravimetrically with a semimicroanalytical balance to obtain high precision and accuracy. Weights of aliquots were converted to volumes by using the density of the buffer solution which was determined with an Anton–Parr precision densimeter. The presence of the protein and of vinblastine had very little effect on the solution density and was ignored in the calculations. The internal or excluded volume of the gel was determined by using Blue Dextran 2000. Three milliliters of Blue Dextran 2000 (0.02–0.2%) was added to each tube containing 100 mg of the dried gel. The gel was indubated for 20 h at room temperature. An aliquot was then taken from the supernatant for measurement of the Blue Dextran concentration from its UV absorbance at 260 nm. The internal volume of the gel was also determined by using a tubulin solution and measuring the protein concentration spectrophotometrically as described above for the control experiments. The results obtained by this method differed by less than 5% from the values obtained with the Blue Dextran 2000, indicating nearly complete exclusion of the protein from the internal volume of the gel.

Calculation of Vinblastine Binding to Tubulin. Assuming complete exclusion of the Blue Dextran 2000 from the internal phase of the gel, the internal volume per unit weight of the gel $\bar{V}_i$ can be calculated from

$$A_e/A = V_t/V_e \quad (1)$$

$$V_t = V_e + V_i \quad (2)$$

$$\bar{V}_i = V_i/g \quad (3)$$

where A and A_e are the absorbance at 260 nm of Blue Dextran 2000 in the stock solution and the external phase, respectively,

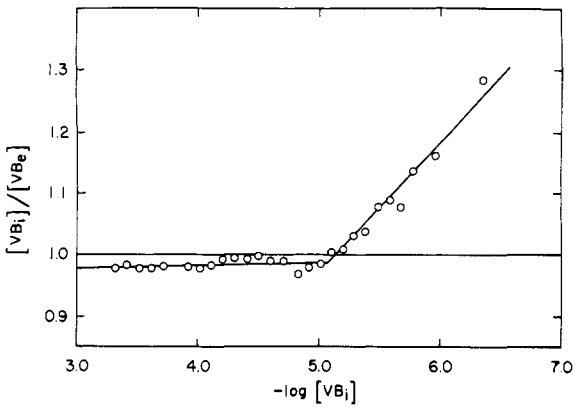

FIGURE 1: Adsorption of [^{3}H]vinblastine to Bio-Gel P-100. Bio-Gel P-100 was swollen in PG buffer for 24 h as described under Materials and Methods. [^{3}H]Vinblastine was then added, and the mixture was incubated at 20 °C for another 1 h before aliquots were removed for radioactive scintillation counting. The calculation of vinblastine concentrations in the internal and external phases of the gel is described in the text. The data were fitted by least squares to two straight lines, from 10^{-7} to 10^{-5} M vinblastine and from 10^{-5} to 10^{-3} M vinblastine.

V_e is the external volume, V_i is the internal volume, and g is the weight of the gel. $\bar{V}_i$ had a value of 9.16 ± 0.10 mL/g for the Bio-Gel P-100 used. For a given sample used in the determination of vinblastine binding, the volumes of the internal and external phases of the gel were calculated according to eq 2 and 3. $[VB_i]$, the concentration of the ligand in the internal phase of the gel, was calculated from

$$[VB_i] = \{(VB) - [VB_e]V_e\}/V_i \quad (4)$$

where (VB) is the total amount of vinblastine added and $[VB_e]$ is the concentration of vinblastine in the external volume. In an ideal case, the concentration of the free ligand in the external phase of the gel should be equal to the concentration of the ligand in the internal phase of the gel; i.e., the partition coefficient of the free ligand should be equal to one. For vinblastine, however, $[VB_i]$ was found to be different from $[VB_e]$.

Two types of gel, Bio-Gel and Sephadex, were tested. Both gels showed some adsorption of [^{3}H]vinblastine in the absence of tubulin. Bio-Gel, however, showed less adsorption than Sephadex, possibly due to the difference in the chemical structures of the gel matrices. Furthermore, the adsorption decreased with increasing porosity of the gel. Consequently, Bio-Gel P-100, the largest pore size Bio-Gel that still excludes tubulin, was chosen for the experiments. The adsorption of the ligand to the gel was time-dependent. Within 1 h of incubation, the adsorption of the drug was minimal and reproducible. This led to the experimental protocol in which the gel was swollen without the drug and the drug was allowed to be in contact with the gel for only 1 h before aliquots were removed for measurements of the binding. Figure 1 depicts the adsorption of [^{3}H]vinblastine to Bio-Gel P-100 in the absence of tubulin. It is evident that above 10^{-5} M vinblastine, the fraction of the drug adsorbed to the gel matrix was small. In fact, above 1×10^{-5} M vinblastine the partition coefficient of vinblastine, defined as $[VB_i]/[VB_e]$, was somewhat less than one, suggesting that vinblastine molecules cannot penetrate some internal volume of the gel that is accessible to water molecules. This is most likely due to the bulkiness of the drug molecule which has a molecule weight of 960. Below 1×10^{-5} M, the fraction of vinblastine adsorbed to the gel became significant, and the $[VB_i]/[VB_e]$ ratio increased linearly as a function of log $[VB_i]$. To correct for this nonideality, which is due either to the exclusion of the drug from some internal

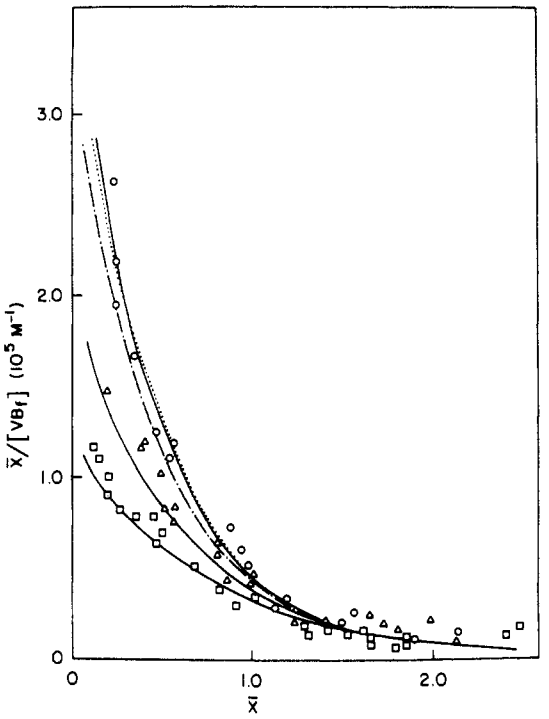

FIGURE 2: Scatchard plots of the binding of vinblastine to calf brain tubulin in PG buffer at 20 °C. The protein concentrations were 1.6×10^{-5} (□), 3.4×10^{-5} (△), and 7.8×10^{-5} M (○). The solid curves are least-squares fittings of the data by the theoretical binding isotherms calculated for the one-ligand-mediated plus -facilitated self-association mechanism as described in the text. The intrinsic association constants used were as follows: $K_1 = 4 \times 10^4$ M^{-1}, $K_2 = 1.8 \times 10^5$ M^{-1}, $K_3 = 4 \times 10^6$ M^{-1}, $K_4 = 1.8 \times 10^3$ M^{-1}, $n_0 = 2$, and $K_0 = 5 \times 10^3$ M^{-1}. Two additional binding isotherms were calculated for the protein concentration of 7.8×10^{-5} M by using the same values of K_1, K_2, n_0, and K_0 but different K_3 and K_4: $K_3 = 1 \times 10^6$ M^{-1} and $K_4 = 7.2 \times 10^3$ M^{-1} (–·–); $K_3 = 4 \times 10^7$ M^{-1} and $K_4 = 1.8 \times 10^2$ M^{-1} (···).

volume of the gel or to the adsorption of the drug to the gel matrix, all data were corrected according to Figure 1 through interpolation. By assuming that the distribution of the free drug is unaffected by the presence of the protein, i.e., that the concentration of the drug in the internal volume of the gel depends only on the concentration of the free drug in the external phase of the gel, one can obtain $[VB_f]$, the concentration of the free drug in the external phase, from $[VB_i]$ by interpolation. In this manner, the concentration of vinblastine bound to tubulin in the external volume was calculated with

$$[VB_b] = [VB_e] - [VB_f] \quad (5)$$

RESULTS

Vinblastine–Tubulin Interaction. Figure 2 shows the Scatchard plots of the binding of vinblastine to tubulin measured at three different protein concentrations by the batch gel filtration method. The results indicate unequivocally the presence of at least two vinblastine binding sites on the protein, with an uncertain number of additional sites evidenced by stoichiometries of >2 at all three protein concentrations examined. Furthermore, the points at stoichiometries of <2 do not extrapolate clearly to two. The binding data show a strong dependence on tubulin concentration. The isotherm obtained at 1.6×10^{-5} M tubulin was slightly curved upward. At the higher protein concentrations of 3.4×10^{-5} M and 7.8×10^{-5} M, the binding isotherms curved upward progressively much more strongly. This change in the binding isotherm with an increase in protein concentration is related only to the binding of the first vinblastine molecule. The apparent association

Scheme I

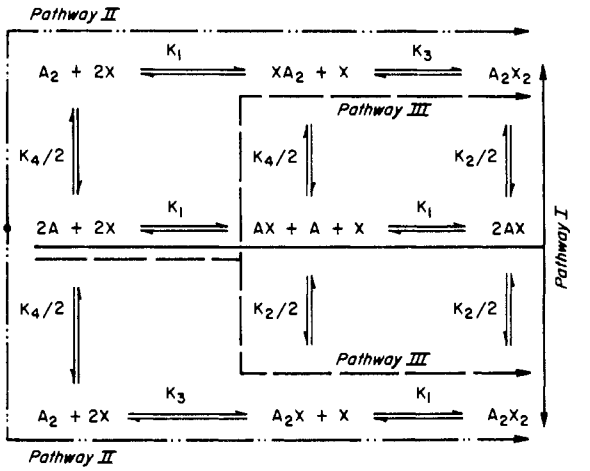

constant of the first site, as reflected by the intercept on the ordinate of the plot, increased 3-fold as the protein concentration was raised from 1.6×10^{-5} to 7.8×10^{-5} M. The binding of vinblastine to the rest of the sites, however, was little affected by the increase in tubulin concentration.

Analysis of Vinblastine–Tubulin Binding Data. The vinblastine–tubulin binding isotherms presented above were analyzed quantitatively through fitting to theoretically calculated isotherms. Since the results shown in Figure 2 indicated that the binding of only the first vinblastine molecule per tubulin α–β dimer is significantly affected by the change in protein concentration, the data analysis was focused on the one-ligand-induced self-association mechanism. For a one-ligand-induced macromolecular self-association, one can devise essentially unlimited varieties of equilibrium linkages. Here we will concentrate on three of the simplest models that have been examined previously in the linked function analysis of the vinblastine-induced tubulin self-association (Na & Timasheff, 1980b). These are shown in Scheme I. In Scheme I, A and X denote the macromonomer and the ligand, respectively. This scheme expresses only the dimerization reaction, although the self-association can be extended easily to higher stoichiometries while the same ligand linkage mechanism is still maintained. In this scheme, pathway I represents a ligand-mediated self-association, while pathway II is the ligand-facilitated self-association (Cann & Kegeles, 1974). The following section presents fittings of the vinblastine–tubulin binding data by the various theoretical isotherms. The equations used in calculating the theoretical isotherms are described in detail in the Appendix.

(*1*) *Ligand-Mediated Self-Association.* This association mechanism as represented by pathway I of Scheme I is defined as one in which the macromonomer must first bind the ligand before self-associating. Scatchard binding isotherms calculated at different protein concentrations for a ligand-mediated isodesmic indefinite self-association using eq 7a–9a are depicted in Figure 3. In this calculation it was assumed that each macromonomer carries a self-association-linked ligand binding site. To obtain an initial estimate of the intrinsic ligand binding constant of this site (K_1), the intercepts on the ordinate of the Scatchard plots of vinblastine–tubulin binding were obtained from Figure 2 and plotted against the protein concentration as shown in Figure 4. The intercept increases with increasing protein concentration, which, according to eq 5a, indicates that the vinblastine-induced tubulin self-association cannot be fitted by the ligand-mediated self-association mechanism. To carry out the calculation of the theoretical ligand binding isotherm, the three data points of Figure 4 were extrapolated linearly

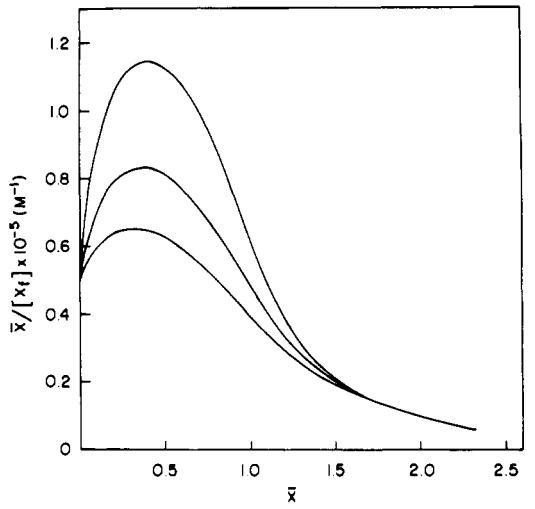

FIGURE 3: Scatchard plots of ligand binding for a ligand-mediated isodesmic indefinite self-association. The details of the association scheme are described in the text. The macromolecular concentrations used, starting from the bottom, are as follows: 1.6×10^{-5}, 3.4×10^{-5}, and 7.8×10^{-5} M. The intrinsic association constants used were as follows: $K_1 = 4 \times 10^4$ M^{-1}, $K_2 = 1.8 \times 10^5$ M^{-1}, $n_0 = 2$, and $K_0 = 5 \times 10^3$ M^{-1}.

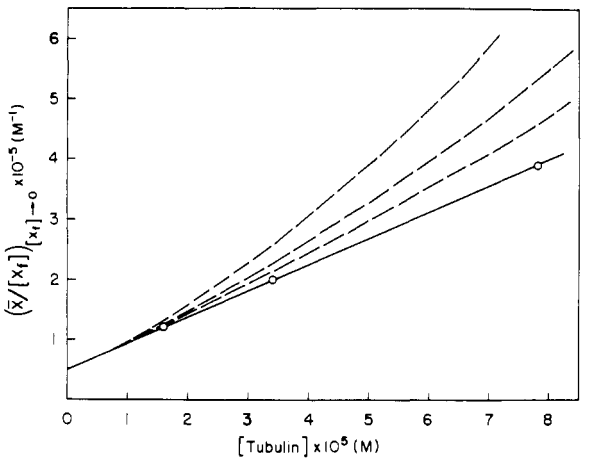

FIGURE 4: Dependence of the intercepts on the ordinate of the Scatchard plots of Figure 2 on total protein concentration. The solid line is the linear least-squares fitting of the data. Using eq 20a and assigning $n_0K_0 = 1 \times 10^4$ M^{-1}, this straight line gave $K_1 = 4 \times 10^4$ M^{-1} and $K_2 + K_4 = 2 \times 10^5$ M^{-1}. The dashed lines were calculated with eq 19a by using the same parameters except for K_4, which was given values of, from the bottom up, 2.5×10^3 M^{-1}, 5×10^3 M^{-1}, and 1×10^4 M^{-1}.

to zero protein concentration, which gave an intercept of 5×10^4 M^{-1} on the ordinate. Consequently, K_1 was given the value of 4×10^4 M^{-1}, and a provision was made according to eq 5a that each macromonomer also carries two self-association-independent sites with identical constants of 5×10^3 M^{-1}. The self-association constant between two liganded monomers (K_2) was assigned the value of 1.8×10^5 M^{-1}, which was obtained from the earlier study of the vinblastine-induced tubulin self-association (Na & Timasheff, 1980b). Since the ligand affinities of the self-association-independent binding sites are much weaker than that of the association-linked site, their presence has very little effect on the left-hand portion of the isotherm where the stoichiometry is less than 1. In that region, the binding isotherms approach a straight line at low protein concentration. As the protein concentration increases, however, they become increasingly concave downward. Above 1×10^{-5} M protein, a maximum appears in the isotherms between ligand stoichiometries of 0.3 and 0.5. All binding isotherms

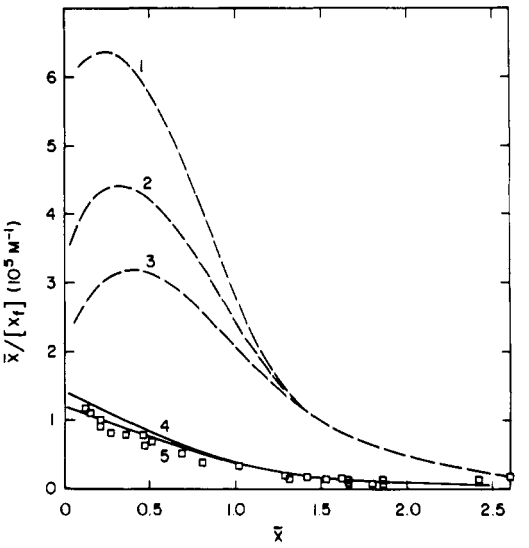

FIGURE 5: Scatchard plots of ligand binding for a one-ligand-facilitated isodesmic indefinite self-association. The details of the association scheme are described in the text. The squares represent the same data as in Figure 2 obtained at 1.6×10^{-5} M tubulin. The macromolecule concentrations are 7.8×10^{-5} M for curves 1 and 4, 3.4×10^{-5} M for curve 2, and 1.6×10^{-5} M for curves 3 and 5. For the two sets of theoretical isotherms, the association parameters are as follows: $K_3 = 2.44 \times 10^6$ M^{-1}, $K_4 = 1.8 \times 10^3$ M^{-1}, $n_0 = 2$, and $K_0 = 2.5 \times 10^4$ M^{-1} (---); and $K_3 = 1.4 \times 10^5$ M^{-1}, $K_4 = 1.5 \times 10^5$ M^{-1}, $n_0 = 2$, and $K_0 = 5 \times 10^3$ M^{-1} (—).

have the same intercept on the ordinate, which corresponds to $K_1 + n_0K_0$, i.e., the sum of the intrinsic ligand binding constants of all the available binding sites. n_0 and K_0 are the stoichiometry and association constant of the self-association-independent ligand binding site (see eq 5a).

The vinblastine–tubulin binding data, shown in Figure 2, obviously do not display any downward curvature, which excludes the possibility that the self-association proceeds solely through a ligand-mediated mechanism. Consequently, no attempt was made to refine the initial approximations of the association parameters.

(2) Ligand-Facilitated Self-Association. A ligand-facilitated self-association is defined as one in which the ligand binds only to the polymers. A one-ligand-facilitated dimerization is depicted by pathway II of Scheme I. Notice that the model described by Scheme I assumes two different ligand binding constants for the two association-linked sites on the dimer, K_1 and K_3. We shall consider a simpler version of one-ligand-facilitated isodesmic indefinite self-association having the same intrinsic ligand binding constant for all the association-linked ligand binding sites on the polymer (K_3) and the same intrinsic association constant for the self-association between unliganded monomers (K_4). Analysis of the vinblastine–tubulin binding data by such an association scheme started with fitting the protein concentration dependence of the intercept on the ordinate of the Scatchard plot (Figure 4) with eq 14a. Such a fitting gave $K_3K_4 = 4.4 \times 10^9$ M^{-2} and $n_0K_0 = 5 \times 10^4$ M^{-1}. From earlier sedimentation velocity studies it is known that, if the ligand-facilitated self-association is operative, K_4 must be $<1.8 \times 10^3$ M^{-1} (Na & Timasheff, 1980b). Taking an initial estimate of $K_4 = 1.8 \times 10^3$ M^{-1} gives $K_3 = 2.44 \times 10^6$ M^{-1}. Also, $K_0 = 2.5 \times 10^4$ M^{-1} assumes that $n_0 = 2$. The ligand binding isotherms calculated by using these association parameters and the same macromolecule concentrations as those used in measuring the vinblastine–tubulin bindings are depicted by the dashed curves in Figure 5. Similar to the ligand-mediated self-association, the binding isotherms for the ligand-facilitated self-association are also concave downward.

However, they do not converge at the ordinate. As the macromolecule concentration increases, the apex of the isotherm gradually shifts leftward. Consequently, by increasing the macromolecule concentration, the isotherm eventually loses its downward curvature.

The vinblastine–tubulin binding data shown in Figure 2 obviously do not display the type of curvature predicted for the ligand-facilitated self-association system. Two major disagreements are evident. First, the left-hand side of the theoretical isotherms ($\bar{X} < 1$), which is contributed mainly by the self-association-linked site, was too high, and it curved downward instead of upward. Second, the right-hand side of the isotherm ($\bar{X} > 1$), which is contributed mainly by the self-association-independent sites, was also too high. Fitting of the experimental data requires that the association parameters be changed. The left-hand side of the theoretical isotherm can be lowered and made to be concave upward by decreasing the value of K_3 and increasing the value of K_4. The right-hand side of the theoretical isotherm can be lowered by reducing the value of K_0. A resulting theoretical isotherm calculated after such changes that can fit reasonably well the experimental data at 1.6×10^{-5} M tubulin is shown by curve 5 of Figure 5. However, this theoretical isotherm requires $K_4 = 1.5 \times 10^5$ M^{-1}, which is inconsistent with the earlier results of the sedimentation velocity studies (Na & Timasheff, 1980b). Moreover, as shown by curve 4 of Figure 5, the theoretical isotherms calculated by using these association parameters do not change much with increasing macromolecule concentration and, consequently, cannot fit the data obtained at the two higher tubulin concentrations. This is due to the fact that a strong K_4 makes the apparent ligand binding approach the intrinsic ligand binding (K_3). In view of the overall inconsistency, the ligand-facilitated mechanism was rejected for the vinblastine-induced tubulin self-association.

(*3*) *Ligand-Mediated plus -Facilitated Self-Association.* This mechanism is defined as a combination of the above two mechanisms; i.e., ligand can bind to both monomers and polymers, and both liganded and unliganded monomers can participate in the self-association reaction. A one-ligand-mediated plus -facilitated dimerization reaction is shown by the full Scheme I. Pathway III permits the self-association between a liganded and an unliganded monomer. This pathway assumes an asymmetry in the self-association; i.e., when two monomers self-associate, the association constant is dependent on the liganding state of only one of them. If the monomer is liganded, the association constant is K_2. If it is unliganded, the association constant is K_4.

The theoretical binding isotherm for such an association scheme can be calculated from either eq 16a or eq 17a. The actual fitting of the binding isotherms was started by obtaining a set of estimated values for the intrinsic association constants. The dependence of the intercepts on the ordinate of the Scatchard plots of Figure 2 on total protein concentration, shown in Figure 4, is linear and can be fitted well by eq 20a. According to eq 20a, in order to obtain the intrinsic association constants from the slope and intercept on the ordinate of Figure 4, one must know the value of n_0K_0. From Figure 2, it is evident that these self-association independent sites were not saturated even at the highest drug concentration studied, rendering it impossible to determine their exact stoichiometry and association constant. One can, however, estimate that $n_0K_0 = 1 \times 10^4$ M^{-1} (see Figures 3 and 5). Assuming $K_4 = 0$, i.e. that pathway II is absent, one obtains initial estimates of $K_1 = 4 \times 10^4$ M^{-1} and $K_2 = 2.2 \times 10^5$ M^{-1}. Introduction of these intrinsic association constants into eq 19a gives the straight line shown in Figure 4, which fits the data quite well. If a nonzero value of K_4 is used in eq 19a, the dependence of the Scatchard intercept on the ordinate on total protein concentration becomes curvilinear, as depicted by the dashed lines of Figure 4.

The actual least-squares fittings of the binding of vinblastine to tubulin, shown in Figure 2, were carried out by using the above values as initial approximations, and the final best fitted results are depicted by the solid lines in Figure 2. The best fitted values for the intrinsic association constants are $K_1 = 4 \times 10^4$ M^{-1} and $K_2 = 1.8 \times 10^5$ M^{-1}. The values of K_3 and K_4 were 4×10^6 M^{-1} and 1.8×10^3 M^{-1}. Two additional theoretical isotherms were calculated for the total protein concentration of 7.8×10^{-5} M by using the above values of K_1 and K_2 but different values of K_3 and K_4. They are depicted by the dashed and dotted lines. Their purpose was to demonstrate that the binding isotherm remains unchanged once K_3 is $>10^6$ M^{-1}. According to eq 15a and 16a, decreasing K_4 to near zero and increasing K_3 to infinity are equivalent to eliminating pathway II. Thus, the vinblastine binding data of Figure 2 can be fitted best by either the combined association pathways I and III or pathways I–III with $K_4 = 2 \times 10^3$ M^{-1} and $K_3 = 2 \times 10^6$ M^{-1}.

Discussion

The present detailed study of the binding of vinblastine to tubulin, taking cognizance of the linked protein self-association reaction, has led to the conclusion that each tubulin α–β dimer has one specific vinblastine binding site, with an intrinsic binding constant $K_1 = 4 \times 10^4$ M^{-1}. The binding of vinblastine is linked to the self-association, the binding constant to polymerized tubulin being $K_3 \geq 4 \times 10^6$ M^{-1}. Vinblastine can bind to tubulin at additional sites, probably nonspecific, with a binding constant $K_0 \leq 5 \times 10^3$ M^{-1}. The number of these sites n_0 is uncertain, there being a minimum of 2. The data, however, set a limit on the product n_0K_0 at 1×10^4 M^{-1}. This binding stoichiometry is different from the one reported previously that there are two specific vinblastine binding sites per α–β tubulin dimer (Wilson et al., 1975; Lee et al., 1975; Bhattacharyya & Wolf, 1976), with essentially identical binding constants (Lee et al., 1975; Wilson et al., 1975). This early conclusion on the binding stoichiometry must be regarded as incorrect and is here withdrawn by one of us (S.N.T.). The value of the intrinsic binding constant, however, remains essentially unchanged. There are two principal reasons for the earlier incorrect conclusion concerning the stoichiometry. First, in the study from this laboratory (Lee et al., 1975), the binding stoichiometry was obtained from a Scatchard plot analysis of data obtained by the Hummel–Dreyer gel filtration method. As discussed below, this method cannot be used with systems in which the binding is linked to self-association and is, therefore, protein concentration dependent. Second, in the study from this laboratory (Lee et al., 1975), the data points stopped at a binding stoichiometry $\bar{X}$ of 1.5 mol vinblastine per α–β tubulin dimer, which precluded detection of binding beyond 2 sites. Similar arguments can be applied to the data from Wilson's laboratory (Wilson et al., 1975). The problems with the data of Bhattacharyya and Wolff (1976) will be discussed in the following paper (Na & Timasheff, 1986). The remainder of the thermodynamic analysis of the binding given in the paper of Lee et al. (1975) remains valid since the measurements were done by fluorescence perturbation at very low protein concentration, where the extent of self-association is negligible.

Multiple equilibria in a ligand-induced macromolecular self-association system can be analyzed by two different ap-

proaches. The first approach involves measuring at constant ligand activity the stoichiometry and apparent association constants of the macromolecular self-association. The apparent association constants obtained can be analyzed further as a function of the ligand activity in order to elucidate the equilibrium linkage between the ligand binding and the self-association reactions. The second approach in characterizing a ligand-induced macromolecular self-association is through the measurement and analysis of ligand binding isotherms at constant concentrations of the macromolecule. Theoretical binding isotherms can be calculated for ligand-induced macromolecular self-associations (Cann & Hinman, 1976; Nichol & Winzor, 1976; Cann, 1978). Since these exhibit different characteristic shapes depending on the ligand stoichiometries and the linkage mechanisms, analysis of the ligand binding data by fitting them with theoretically calculated isotherms can also diagnose the equilibrium linkages of the system.

These two types of studies usually utilize different experimental methods, one that measures the self-association of the macromolecules and another that determines ligand binding. They are, therefore, independent of each other with respect to the nonidealities present in the experimental method and the assumptions involved in the data analysis. Consequently, by taking the two approaches, one can gain stronger confidence in the derived conclusions. Furthermore, these two approaches complement each other well, and intrinsically each has its own advantages and drawbacks. For instance, when the equilibrium linkage is probed by analysis of the apparent self-association constant, information is obtained only on the self-association-linked ligand binding site(s), but nothing is learned about the self-association independent site(s). On the other hand, the ligand binding study provides information on all the ligand binding site(s) on the protein, but the shape of the theoretical ligand binding isotherm is usually not sensitive to the stoichiometry of the self-association reaction (Cann & Hinman, 1976). The complementary use of these two approaches is demonstrated in the present study, in which an isodesmic indefinite mechanism for the self-association, which had been deduced from earlier sedimentation velocity studies, was adopted for the analysis of the ligand binding isotherms.

It is important to note that, while both approaches probe the linkage mechanism, each emphasizes a specific region of the binding isotherm. To illustrate this, let us examine the previously reported sedimentation velocity study of the vinblastine-induced tubulin self-association (Na & Timasheff, 1980b), which constitutes the first type of approach described above. In that study, the data analysis was focused on the region where the association-linked ligand binding site was half to fully saturated. The plateau of the self-association at saturating ligand concentrations indicated the presence of a ligand-mediated association mechanism. It also ruled out the possibility that a ligand-facilitated self-association was the only association pathway, since for this association mechanism K_2^{app} should not plateau at high ligand concentrations. A plot of ln K_2^{app} as a function of ln $[X_f]$ gave a slope of 0.95 at low ligand concentration, indicating that each step of the self-association is accompanied by the binding of one vinblastine molecule. It should be noted that that study was not effective in proving the presence or absence of a weak ligand-facilitated self-association. One can easily detect the presence of a strong ligand-facilitated self-association, since it causes a plateau of the above logarithmic plot at low ligand concentrations. If the apparent self-association constant continues to decrease at the lowest ligand concentration studied, however, as is true in the vinblastine-induced tubulin self-association, it is impossible to rule out the presence of a weak ligand-facilitated pathway that is beyond detection by the technique used (Na & Timasheff, 1980b). Nevertheless, in fitting experimental data with theoretical models, it is best to observe the rule of choosing the simplest model that can accommodate the data. For the vinblastine-induced tubulin self-association, the simplest model that could accommodate the sedimentation velocity data was that of an isodesmic indefinite association with the linkage mechanism shown by pathways I and III of Scheme I without pathway II being invoked. A fit of the experimental data to that model gave $K_1 = 1.8 \times 10^4$ M^{-1} and $K_2 = 1.8 \times 10^5$ M^{-1}.

In juxtaposition to the self-association study, a probe of the linkage mechanism through analysis of ligand binding, as was carried out in the present study, is focused on the region where the association-linked ligand binding site is less than half-saturated. It is in this region that different linkage mechanisms manifest most pronounced differences in the shapes of their binding isotherms. Yet, good quality ligand binding data can be obtained still, permitting differentiation between these linkage mechanisms. As shown in Figures 2 and 3, the upward curvature of the vinblastine–tubulin binding data suggested that the ligand-mediated self-association could not be the only reaction pathway for the vinblastine-induced tubulin self-association. The data fit by the ligand-facilitated pathway, shown in Figure 5, was also poor. The results shown in Figures 2 and 4 demonstrated, however, that the vinblastine to tubulin binding isotherms can be fitted quite well by the one-ligand-induced isodesmic indefinite self-association mechanism with an equilibrium linkage mechanism described by pathways I and III of Scheme I, although the possibility of the simultaneous presence of pathway II with a weak K_4 could not be ruled out. This is fully consistent with the conclusions drawn from the sedimentation velocity study of the self-association reaction. Quantitatively, the intrinsic association constants derived in the present binding study are similar to those obtained from the self-association study, although in the present study K_1 has a value of 4×10^4 M^{-1}, which is higher than the value of 1.8×10^4 M^{-1} obtained in the sedimentation velocity study (Na & Timasheff, 1980b). This minor discrepancy can be attributed to the different nonidealities inherent in the physical techniques used and the different assumptions invoked in the data analyses. The K_2 values obtained from the two approaches are identical. It should be noted that in the sedimentation velocity study the value of K_2 was obtained at saturating ligand concentration. It should, therefore, correspond to the self-association constant between two fully liganded monomers. On the other hand, in the present study the value of K_2 was obtained at zero ligand concentration. In eq 18a, K_2 is contributed by the second term and corresponds to twice the self-association constant between a liganded monomer and an unliganded one. The factor of 2 is a statistical one. It is interesting to note that this factor was borne out exactly by the experimental data.

The good straight-line fit of the points of Figure 4 indicates that K_4 must be small. This is consistent with the curve fitting shown in Figure 2. The three binding isotherms calculated for a total protein concentration of 7.8×10^{-5} M demonstrate that, for a given set of K_1 and K_2, the apparent ligand bindings changed very little between $K_3 = 4 \times 10^6$ and 4×10^7 M^{-1}. This is due to the fact that, when $K_4 < 2 \times 10^3$ M^{-1}, the ligand binding contributed by pathway II becomes insignificant relative to the other two pathways. Consequently, the above best fitted values of K_3 and K_4 should be taken only as lower and upper limits. Beyond these limits, the theoretically cal-

culated curve for Figure 5 becomes curvilinear and the isotherms calculated for Figure 2 become so concave that the fitting starts to deteriorate.

The data of Figure 2 also showed that the binding of vinblastine to tubulin beyond the first binding site is not affected by a change in protein concentration and is, thus, independent of the self-association reaction. This is consistent with the earlier findings that the self-association proceeds upon the binding of one vinblastine molecule to each tubulin α–β dimer (Na & Timasheff, 1980b). The binding of vinblastine to these self-association-independent sites is weak, and they do not become saturated even at the highest drug concentration studied. Consequently, the stoichiometry and binding constant for these sites are only approximations. This weak binding of vinblastine to tubulin may well be nonspecific, in view of the fact that vinblastine interacts nonspecifically with a large number of proteins, causing them to precipitate out of solution (Wilson et al., 1970).

Finally, a word is needed to justify the choice of the batch gel filtration method for the determination of the binding of vinblastine to tubulin. This choice was dictated by two requirements. First, the measurements must be conducted at conditions of equilibrium; i.e., the binding must reflect the true equilibrium state of the reaction. Second, in a self-association-linked binding study the protein concentration must be controlled precisely, so that each binding point corresponds to an exact known protein concentration and each isotherm is determined at a constant protein concentration. These requirements rule out several techniques that have been used in the past in studies of the binding of vinblastine to tubulin. These include Hummel–Dreyer column chromatography (Lee et al., 1975; Wilson et al., 1975) and the use of ion-exchange resin impregnated paper disks (Bhattacharyya & Wolff, 1976). The Hummel–Dreyer method does measure ligand binding under equilibrium conditions (Hummel & Dreyer, 1962), but the results are expressed as ligand binding across the total protein peak, instead of at a given protein concentration. Therefore, it is not suitable for a protein concentration dependent study. In the ion-exchange resin-impregnated disk method, the disks need to be washed extensively after application of the protein to remove the unbound ligand. For rapidly reequilibrated association–dissociation systems, such as the vinblastine–tubulin interaction, this leads to nonequilibrium results.

The batch gel filtration method is, in fact, quite similar to equilibrium dialysis, except that a porous gel is used in place of a semipermeable membrane. Compared to equilibrium dialysis, the batch gel filtration method requires much less material and gives a better control of protein concentration. However, similarly to equilibrium dialysis, it is frequently complicated by adsorption of ligand to the gel matrix (Gellote, 1960; Johnson, 1967; Pearlman & Crêpy, 1967). This makes it necessary to correct the data by determining a complete binding isotherm between the ligand and the gel matrix in the absence of the protein.

Appendix

Calculation of Theoretical Ligand Binding Isotherms of Ligand-Induced Self-Association Systems. For a ligand-induced self-association, the binding of the ligand to the macromolecule, irrespective of the reaction pathway, can be expressed in the Scatchard format as

$$\frac{\bar{X}}{[X_f]} = \frac{[X_b]}{[A_t][X_f]} = \frac{\sum_{i=1}^{n}\sum_{j=1}^{m} j[A_iX_j]}{[A_t][X_f]} \qquad (1a)$$

where $[X_b]$ and $[X_f]$ refer to the concentrations of the bound and free ligand, respectively, $[A_t]$ is the total concentration of the macromolecule expressed as monomers, and $[A_iX_j]$ is the concentration of the i-mer containing j bound ligand molecules. Let us examine, in turn, the ligand binding pattern expected for each individual association pathway expressed in Scheme I:

(*1*) *Ligand-Mediated Self-Association.* A one-ligand-mediated self-association is described by pathway I of Scheme I. If the linkage mechanism is extended to an isodesmic indefinite one, the apparent self-association constant K_2^{app} can be expressed as (Na & Timasheff, 1980b)

$$K_2^{app} = \frac{[A_2X_2]}{([A] + [AX])^2} = \frac{K_1^2K_2[X_f]^2}{(1 + K_1[X_f])^2} \qquad (2a)$$

where $[X_f]$ is the concentration of the free ligand and K_1 and K_2 have the same definitions as in Scheme I. By setting $j = i$ and $m = n$ in eq 1a, one obtains

$$\frac{\bar{X}}{[X_f]} = \frac{\sum_{i=1}^{n} iK_1^iK_2^{i-1}[A_f]^i[X_f]^{i-1}}{[A_t]} \qquad (3a)$$

where $[A_f]$ is the concentration of unliganded monomers. The contribution of the self-association-independent ligand binding sites to the total bound ligand can be expressed as, assuming that these sites are all of equal affinity

$$[X_b] = \frac{n_0K_0[X_f][A_t]}{1 + K_0[X_f]} \qquad (4a)$$

where n_0 is the total number of such sites and K_0 is their ligand binding constant. Consequently

$$\lim_{[X_f]\to 0} (\bar{X}/[X_f]) = K_1 + n_0K_0 \qquad (5a)$$

which means that the intercept on the ordinate of the Scatchard plot is $K_1 + n_0K_0$, regardless of the total protein concentration used.

To calculate the actual binding isotherms from eq 3a, one needs first to obtain $[A_f]$, the free monomer concentration. If the self-association is an isodesmic indefinite one, the total monomer concentration is given by (Na & Timasheff, 1980a)

$$[A_1] = \frac{(2K_2^{app}[A_t] + 1) - \sqrt{4K_2^{app}[A_t] + 1}}{2(K_2^{app})^2[A_t]} \qquad (6a)$$

The unliganded monomer concentration is then

$$[A_f] = \frac{[A_1]}{1 + K_1[X_f]} \qquad (7a)$$

where $[A_1]$ is the total concentration of the monomer. Given $[A_t]$, $[X_f]$, K_1, and K_2, the values of K_2^{app}, $[A_1]$, and $[A_f]$ can be calculated from eq 2a, 6a, and 7a, and the amount of bound ligand can then be calculated from eq 3a and 4a. The summation of eq 3a proceeds through increments of i until a major portion of the total protein, e.g., 99.9%, has been accounted for. By varying $[X_f]$, the entire Scatchard binding isotherm can be obtained.

Alternately, one can calculate the total concentration of the i-mer according to

$$[A_i] = [A_1]^i(K_2^{app})^{i-1} \qquad (8a)$$

where $[A_i]$ is the total concentration of the i-mer. For a ligand-mediated self-association, all polymers should be fully liganded. As a result

$$\frac{\bar{X}}{[X_f]} = \frac{K_1[A_f][X_f] + \sum_{i=2}^{n} i[A_i]}{[A_t][X_f]} + \frac{n_0K_0}{1 + K_0[X_f]} \quad (9a)$$

(2) *Ligand-Facilitated Self-Association.* A ligand-facilitated dimerization reaction is depicted by pathway II of Scheme I. Here we consider a similar one-ligand-facilitated isodesmic indefinite self-association having the same intrinsic ligand binding constant for all the association-linked ligand binding sites on the polymer (K_3) and the same intrinsic association constant for the self-association between the unliganded monomers (K_4). For such a self-association scheme, the apparent self-association constant can be expressed as

$$K_2^{app} = \frac{[A_2] + [A_2X] + [A_2X_2]}{[A]^2} = K_4 + K_3K_4[X_f] + K_3^2K_4[X_f]^2 \quad (10a)$$

The concentration of the ligand bound to the macromolecule can be expressed as

$$[X_b] = \sum_{i=2}^{\infty}\sum_{j=1}^{i} \frac{i!}{(i-j)!(j-1)!} K_3^j (K_4/2)^{i-1}[A_f]^i[X_f]^j + \frac{n_0K_0[X_f][A_t]}{1 + K_0[X_f]} \quad (11a)$$

where the first term represents the ligand bound to the self-association-linked sites and the second term represents the ligand bound to the self-association-independent sites. Alternately, the ligand bound to the macromolecule can be expressed as

$$[X_b] = \sum_{i=2}^{\infty} \frac{i[A_i]K_3[X_f]}{1 + K_3[X_f]} + \frac{n_0K_0[X_f][A_t]}{1 + K_0[X_f]} \quad (12a)$$

where $[A_i]$ is the total concentration of the i-mer, which can be calculated by using eq 6a, 8a, and 10a. Scatchard binding isotherms for such a one-ligand-facilitated isodesmic indefinite self-association system can be calculated by the same method as described above for the ligand-mediated association systems except that eq 10a and 12a should be used in place of eq 2a and 3a. The data of Figure 4 were used to obtain the initial estimates of the association parameters. According to eq 11a, the intercept on the ordinate of the Scatchard plot for this self-association scheme is

$$\lim_{[X_f]\to 0} \frac{\bar{X}}{[X_f]} = \frac{\sum_{i=2}^{\infty} iK_3(K_4/2)^{i-1}[A_f]^i}{[A_t]} + n_0K_0 \quad (13a)$$

If K_4 is small, at low protein concentrations, $[A_f] = [A_t]$, and eq 13a reduces to

$$\lim_{[X_f]\to 0} (\bar{X}/[X_f]) = K_3K_4[A_t] + \tfrac{3}{4}K_3K_4^2[A_t]^2 + \ldots + n_0K_0 \quad (14a)$$

(3) *Ligand-Mediated plus -Facilitated Self-Association.* The entire Scheme I shows a combined ligand-mediated and -facilitated dimerization reaction. For such a self-association, the apparent dimerization constant can be expressed as

$$K_2^{app} = \frac{[A_2] + [A_2X] + [A_2X_2]}{([A] + [AX])^2} = \frac{K_4 + \tfrac{1}{2}K_1K_2[X_f] + \tfrac{1}{2}K_1K_4[X_f] + K_1^2K_2[X_f]^2}{(1 + K_1[X_f])^2} \quad (15a)$$

If the reaction scheme is extended to a stepwise isodesmic indefinite self-association, the ligand bound to the macromolecule can be expression as

$$[X_b] = \sum_{i=1}^{\infty}\sum_{j=1}^{i} \frac{(i-1)!}{(i-j)!(j-1)!} jK_1^j(K_2/2)^{j-1}(K_4/2)^{i-j}[A_f]^i[X_f]^j + \sum_{i=2}^{\infty}\sum_{j=1}^{i-1} \frac{(i-1)!}{(i-j-1)!(j-1)!} K_1^j(K_2/2)^j(K_4/2)^{i-j-1}[A_f]^i[X_f]^j + \frac{n_0K_0[X_f][A_t]}{1 + K_0[X_f]} \quad (16a)$$

The first term of eq 16a contains macromolecules with the self-association-linked sites fully occupied. This is contributed by pathway I, the ligand-mediated self-association. It also covers polymers with a liganded monomer at the starting end of the polymer. The second term covers polymers with an unliganded monomer at that position. The third term is contributed by the self-association-independent sites. An alternate expression for the concentration of the bound ligand in terms of the concentrations of each i-mer is

$$[X_b] = \sum_{i=2}^{\infty}[A_2]\left\{\frac{K_1[X_f]}{1 + K_1[X_f]} + \frac{(i-1)K_3[X_f]}{1 + K_3[X_f]}\right\} + \frac{n_0K_0[X_f][A_t]}{1 + K_0[X_f]} \quad (17a)$$

According to eq 16a:

$$\lim_{[X_f]\to 0} \frac{\bar{X}}{[X_f]} = \frac{\sum_{i=1}^{\infty} K_1(K_4/2)^{i-1}[A_f]^i + \sum_{i=2}^{\infty}(i-1)K_1(K_2/2)(K_4/2)^{i-2}[A_f]^i}{[A_t]} + n_0K_0 \quad (18a)$$

As the ligand concentration approaches zero, $[A_f]/[A_t] = 1$, and

$$\lim_{[X_f]\to 0} \frac{\bar{X}}{[X_f]} = K_1\left\{1 + \frac{(K_2 + K_4)}{2}[A_t] + \frac{K_4^2 + K_2K_4}{4}[A_t]^2 + \ldots\right\} + n_0K_0 \quad (19a)$$

Neglecting in eq 19a all terms higher than first order in $[A_t]$ gives

$$\lim_{[X_f]\to 0} \frac{\bar{X}}{[X_f]} = K_1\left\{1 + \frac{(K_2 + K_4)}{2}[A_t] + \ldots\right\} + n_0K_0 \quad (20a)$$

Registry No. Vinblastine, 865-21-4.

References

Bensch, K. G., & Malawista, S. E. (1968) *Nature (London) 218*, 1176–1177.

Bensch, K. G., & Malawista, S. E. (1969) *J. Cell Biol. 40*, 95–107.

Bhattacharyya, B., & Wolff, J. (1976) *Proc. Natl. Acad. Sci. U.S.A. 73*, 2375–2378.

Bryan, J. (1971) *Exp. Cell Res. 66*, 129–136.

Bryan, J. (1972a) *Biochemistry 11*, 2611–2616.

Bryan, J. (1972b) *J. Mol. Biol. 66*, 157–168.

Cann, J. R. (1978) *Methods Enzymol. 48*, 299–307.

Cann, J. R., & Kegeles, G. (1974) *Biochemistry 13*, 1868–1874.

Cann, J. R., & Hinman, N. D. (1976) *Biochemistry 15*, 4614–4622.

Fasella, P., Hammes, G. G., & Schimmel, P. R. (1965) *Biochim. Biophys. Acta 103*, 708-710.
Frigon, R. P., & Lee, J. C. (1972) *Arch. Biochem. Biophys. 153*, 587-589.
Gellote, B. (1960) *J. Chromatogr. 3*, 330-342.
Hirose, M., & Kano, Y. (1971) *Biochim. Biophys. Acta 251*, 376-379.
Hummel, J. P., & Dreyer, W. J. (1962) *Biochim. Biophys. Acta 63*, 530-532.
Janson, J.-C. (1967) *J. Chromatogr. 28*, 12-20.
Kegeles, G., & Cann, J. R. (1978) *Methods Enzymol. 48*, 248-270.
Lee, J. C., Frigon, R. P., & Timasheff, S. N. (1973) *J. Biol. Chem. 248*, 7253-7262.
Lee, J. C., Harrison, D., & Timasheff, S. N. (1975) *J. Biol. Chem. 250*, 9276-9282.
Malawista, S. F., & Sato, H. (1969) *J. Cell Biol. 42*, 596-599.
Na, G. C., & Timasheff, S. N. (1980a) *Biochemistry 19*, 1347-1354.
Na, G. C., & Timasheff, S. N. (1980b) *Biochemistry 19*, 1355-1365.
Na, G. C., & Timasheff, S. N. (1980c) American Chemical Society Meeting, Las Vegas, NV, Abstract Biol. 170.
Na, G. C., & Timasheff, S. N. (1981a) *J. Mol. Biol. 151*, 165-178.
Na, G. C., & Timasheff, S. N. (1981b) *Fed. Proc., Fed. Am. Soc. Exp. Biol. 40*, 1548.
Na, G. C., & Timasheff, S. N. (1982) *Methods Enzymol. 85*, 393-408.
Na, G. C., & Timasheff, S. N. (1986) *Biochemistry* (following paper in this issue).
Nichol, L. W., & Winzor, D. J. (1976) *Biochemistry 15*, 3015-3019.
Pearlman, W. H., & Crêpy, O. (1967) *J. Biol. Chem. 242*, 182-189.
Weisenberg, R. C., & Timasheff, S. N. (1970) *Biochemistry 9*, 4110-4116.
Weisenberg, R. C., Borisy, G., & Taylor, E. (1968) *Biochemistry 7*, 4466-4479.
Wilson, L., Bryan, J., Ruby, A., & Mazia, D. (1970) *Proc. Natl. Acad. Sci. U.S.A. 66*, 807-814.
Wilson, L., Creswell, K. M., & Chin, D. (1975) *Biochemistry 14*, 5586-5592.
Wilson, L., Morse, A. N. C., & Bryan, J. (1978) *J. Mol. Biol. 121*, 255-268.

Interaction of Vinblastine with Calf Brain Tubulin: Effects of Magnesium Ions†

George C. Na‡ and Serge N. Timasheff*
Graduate Department of Biochemistry, Brandeis University, Waltham, Massachusetts 02254
Received January 17, 1986; Revised Manuscript Received May 28, 1986

ABSTRACT: The effects of magnesium ions on the binding of the anticancer drug vinblastine to calf brain tubulin were investigated by a batch gel equilibration method. Magnesium ions at 1 mM strongly enhanced the binding of the first vinblastine molecule to each tubulin dimer without affecting either the drug affinity toward the rest of the binding site or the total stoichiometry of the vinblastine binding to tubulin. Sedimentation velocity studies indicated that magnesium ions can enhance strongly the vinblastine-induced tubulin self-association and suggested that the drug-induced self-association still proceeds through the isodesmic indefinite mechanism in the presence of the divalent cation. In PG buffer (0.01 M NaP_i, 10^{-4} M GTP, pH 7.0) containing more than 2.5 mM $MgCl_2$, vinblastine induced tubulin to form large amorphous aggregates. The aggregate formation was rapid and took place at a drug stoichiometry between 0.7 and 1.0 mol of vinblastine per mole of tubulin dimers. Increasing the solution ionic strength decreased the rate of aggregate formation. Between an ionic strength of 0.05 and 0.1, the self-association led to the formation of paracrystalline aggregates instead of the amorphous ones. The results indicated that the binding of only the first vinblastine molecule to each tubulin dimer is linked to the self-association of the protein. They also confirmed our previously proposed rationale for the disagreement among the vinblastine–tubulin binding constants reported in the literature in terms of the different magnesium ion concentrations and ionic strength of the buffers used in the various studies.

In the preceding paper (Na & Timasheff, 1986), we have examined the binding of vinblastine to tubulin as a function of protein concentration and probed the equilibrium linkages between the drug binding and the protein self-association reactions. In that study, in order to simplify the system, magnesium ions were not added to the solution. This rendered vinblastine the only strong ligand effector in the solution. Magnesium ions, however, are known to exert a strong influence on the vinblastine-induced tubulin self-association. Early studies by Weisenberg and Timasheff (1970) had shown that, in the presence of magnesium ions, vinblastine induced the formation of large tubulin aggregates that precipitated from the solution without centrifugation. More recently, we have shown that magnesium ions are required for the in vitro formation of vinblastine–tubulin paracrystals (Na & Timasheff, 1982).

In the analysis of the vinblastine-induced tubulin self-association, we proposed that if magnesium ions can enhance the vinblastine-induced tubulin self-association, they should also enhance the vinblastine binding to the protein, resulting

† This work was supported in part by NIH Grants CA-16707 and GM-14603. This paper is Publication No. 1594 from the Graduate Department of Biochemistry, Brandeis University.
‡ Present address: U.S. Department of Agriculture, Agricultural Research Service, Eastern Regional Research Center, Philadelphia, PA 19118.

0006-2960/86/0425-6222$01.50/0